Macromolecular Research, Vol. 14, No. 4, pp 430-437 (2006)

Ultra-Drawing of Gel Films of Ultra High Molecular Weight Polyethylene/Low Molecular Weight Polymer Blends Containing $BaTiO_3$ Nanoparticles

Ho Sik Park, Jong Hoon Lee, and Jae-Do Nam*

Department of Polymer Science and Engineering, Sungkyunkwan Advanced Institute of Nanotechnology (SAINT), Suwon 440-746, Korea

Soo Jung Seo

Department Metallurgical & Materials Engineering, Sungkyunkwan University, Suwon 440-746, Korea

Young Kwan Lee

Department of Chemical Engineering, Sungkyunkwan University, Suwon 440-746, Korea

Yong Soo Oh and Hyun-Chul Jung

Samsung Electro-Mechanics Co., Ltd., Suwon 443-743, Korea

Received March 14, 2006; Revised June 7, 2006

Abstract: The ultra-drawing process of an ultra high molecular weight polyethylene (UHMWPE) gel film was examined by incorporating linear low-density polyethylene (LLDPE) and $BaTiO_3$ nanoparticles. The effects of LLDPE and the draw ratios on the morphological development and mechanical properties of the nanocomposite membrane systems were investigated. By incorporating $BaTiO_3$ nanoparticles in the UHMWPE/LLDPE blend systems, the ultra-drawing process provided a highly extended, fibril structure of UHMWPE chains to form highly porous, composite membranes with well-dispersed nanoparticles. The ultra-drawing process of UHMWPE/LLDPE dry-gel films desirably dispersed the highly loaded $BaTiO_3$ nanoparticles in the porous membrane, which could be used to form multi-layered structures for electronic applications in various embedded, printed circuit board (PCB) systems.

Keywords: ultra high molecular weight polyethylene (UHMWPE), ultra-drawing, gel film, dispersion, porous membrane.

Introduction

Extensive investigations have been undertaken to devise appropriate methods for processing high performance UHMWPE.[1-10] In order to enhance the drawability of the films and fibers, various methods such as gel drawings,[11] single crystal mat drawings,[12,13] and high-temperature zone drawings[14-18] have been reported. Among these processing methods, the ultra-drawing of specimens prepared by the quenching UHMWPE solutions has attracted a great deal of attention on account of the potential for the commercial production of high strength and high modulus fibers and films, which is often referred to as the gel-deformation method.[2-5,7]

The ultra-drawability of polymers is substantially influenced by intrinsic and extrinsic factors such as the molecular weight,[5,19-21] molecular weight distribution,[22] polymer solution concentration,[2,6] and gelation/crystallization temperatures.[23,24] The ultra-drawability usually increases with increasing molecular weight, and above a certain molecular weight, the ultra-drawability depends primarily on the initial concentration and gelation/crystallization temperature of the polymer solution.[22,24,25] It is believed that these phenomena are associated with the reduced number of entanglements in the solution-cast or solution-spun polymers.[26] The entanglement sites form transient networks as friction centers or junctions and, hence, a high entanglement density at a high concentration or at a low gelation temperature impedes the drawability. In this case, the drawability can be improved by reducing the number of chain entanglements. However, in the case of dilute solutions, which produce fewer entanglements, the maximum draw ratio (DR) decreases because the polymer coils rarely overlap and the polymer chains slip away during the drawing process. Thus, a optimal level of entanglement is needed to attain the maximum draw ratio, for example, by

*Corresponding Author. E-mail: jdnam@skku.edu

controlling the solution concentrations, gelation/crystallization temperatures, etc. Lowering the degree of chain entanglement and viscosity, a low molecular weight polyethylene (LMWPE) has been used to prepare UHMWPE/LMWPE blends to produce high modulus fibers.[5,27-30] The drawability of the UHMWPE gel films may be improved by the incorporation of LMWPE.[28,29,31-34] Such fibers and ultradrawn gel films of UHMWPE/LMWPE blends are important in a commercial point of view because the production rate and the drawability of the gel films are not in the level of commercialization.

In the rapid development of IC technology, one of the most demanding technologies is integration and embedding of different layers of printed circuit boards (PCB) to form a 3D structure, which reduces the size of the circuit but increases its circuit density.[35,36] The current technology is based on high- or low- temperature co-fired ceramic (HTCC or LTCC) processes. Compared with these ceramic-based processes, the polymer-based composite technology has attracted a great deal of attention because it can eliminate complex steps such as firing, flattening, dimensional tolerance control and plating, which are essential in ceramic-based processes. In polymer-based composite processes, by incorporating various nano- and micro-sized functional particles in appropriate polymers, multi-layered composite films can be applied to conductors, resistors, capacitors, inductors and antennas that can further be embedded in a PCB. In these applications, the dispersion of highly-loaded nanoparticles in a polymer matrix and the film-forming process of the polymeric composite are the key issues that should be investigated.

In this study, dielectric $BaTiO_3$ nanoparticles were dispersed in several blended systems containing UHMWPE and low molecular weight polymers, and the dry gel film was ultradrawn up to a draw ratio of 300. The morphological variation of $BaTiO_3$-incorporated UHMWPE blend systems was investigated under a gel-deformation process by examining their thermal and mechanical characteristics.

Experimental

Gel Film Preparation. The polymers used in this study were UHMWPE (Samsung General Chemicals Co., Ltd., Korea) with a viscosity-average molecular weight (M_v) of 4.5×10^6 g/mol, linear low-density polyethylene (LLDPE, Samsung General Chemicals Co., Ltd. Korea) with a melt index (MI) of 1.0, and EPM (ethylene propylene elastomer, KEP 020P grade, Kumho Polychem Co., Ltd., Korea). Mixtures of the low molecular-weight polymers (LLDPE or EPM) and UHMWPE at various weight ratios were dissolved in decahydronaphthalene (decalin, Sigma-Aldrich, 98% mixture of cis and trans) with 0.1 wt% 6-*t*-butyl-*p*-cresol added as an antioxidant at 160 °C. The compositions of UHMWPE and low molecular-weight polymer were 95/5, 90/10, 80/20 and 70/30 by weight, and the concentration of the polymer blend in the solvent was fixed at 1.0 g/100 mL. As a model filler system in this study, $BaTiO_3$ ceramic particles (average particle diameter = 400 nm, Samsung General Chemicals Co.) were mixed with the polymer blend at a composition of polymer blend : decaline : $BaTiO_3$ = 1 : 9 : 1 by weight. The mixture was poured into a glass tray and cooled to room temperature. It was then placed into a vacuum oven for 24 hrs in order to remove the residual trace of decalin. The dry gel films prepared (50-100 μm thick) were cut into 30 mm long and 10 mm wide strips for the film drawing process.

Ultra-Drawing of Specimens. The ultra-drawing of the film specimens was carried out using a tensile tester (Housefield, H100KS) that was equipped with a temperature controlled oven at a crosshead speed of 20 mm/min. The specimens were pre-drawn at various temperatures between 80 and 120 °C to investigate the effect of temperature on the drawability of the UHMWPE blend gel films up to a draw ratio of 3. The pre-drawn films were re-drawn at various draw ratios at 110 °C. The draw ratio was defined as the ratio of the length of the undrawn and drawn specimens, which were measured by the distance marks on the film specimens before and after drawing.

Characterization. The crystalline melting and recrystallization behaviors of the dry gel films and their drawn films were investigated using differential scanning calorimetry (TA Instruments DSC 2910) at a heating rate of 5 °C/min in a nitrogen environment. The orientations of the crystal structures before and after drawing were determined using wide-angle X-ray diffraction (WXRD, RIGAKU Denki Co., Rigaku Rotaflex D/MAX). The applied voltage and current of the X-ray tubes were 30 kV and 100 mA, respectively. The 2θ was scanned between 10 and 35 ° at 2 °/min. The tensile strength and modulus were measured using a tensile tester (Housefield, H100KS) at a deformation speed of 5 mm/min at 25 °C.

Results and Discussion

Melting Behavior. Figure 1(a) and (b), and Table I show that the DSC thermograms of the UHMWPE/low molecular-weight polymer blend films have a single melting peak regardless of the LLDPE and EPM compositions. The heats of melting, crystallization, crystalline melting, and crystallization temperatures were slightly influenced by the incorporation of LLDPE and EPM apparently because they act as defects of crystal. Mixed-crystals have been reported to form during the crystallization of polyethylene mixtures with different molecular weights, and the existence of polyethylene systems has no effect on the degree of UHMWPE crystallinity.[37] It is believed that the low molecular-weight polymers do not have a significant effect on the UHMWPE crystalline melting behavior. However, when the UHMWPE/LLDPE films are drawn, an additional crystalline melting peak is observed at temperatures higher than the

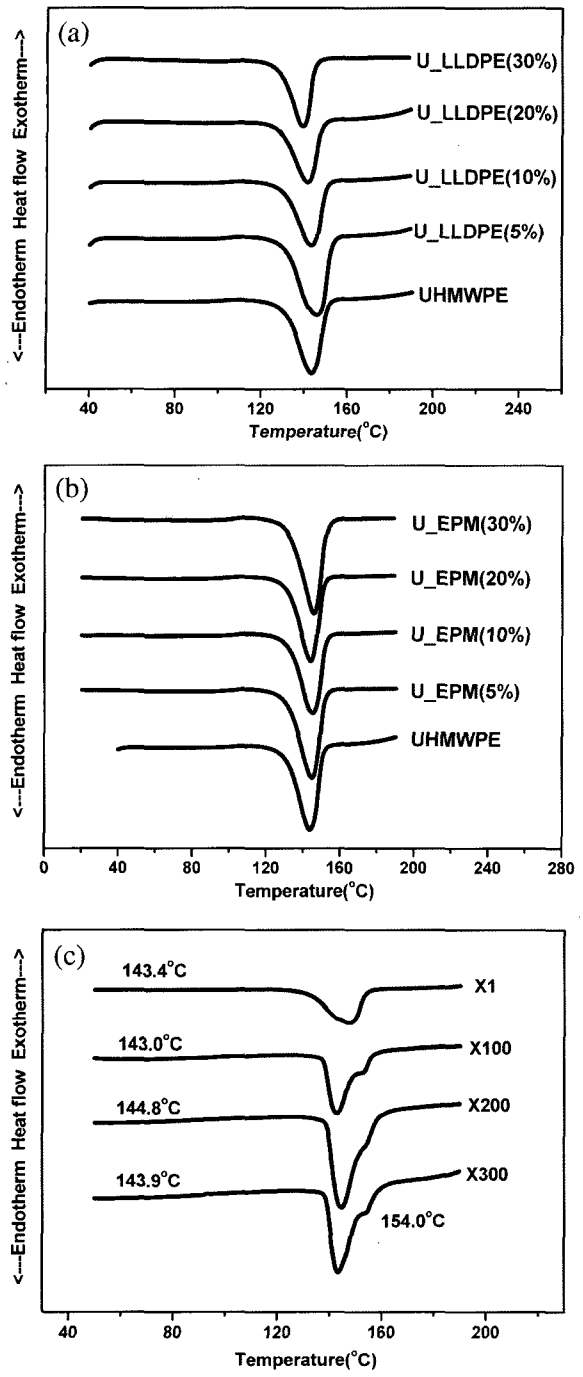

Figure 1. DSC melting thermograms of the UHMWPE/low molecular-weight polymer blend films for various compositions of (a) LLDPE at DR=1 and (b) EPM at DR=1, and (c) HWMWPE/LLDPE (5%) at different drawing ratios. All the thermograms were measured at 10 °C/min in nitrogen.

main melting peak of UHMWPE, as shown in Figure 1(c). According to previous studies,[38,39] three types of crystals namely, fine crystallites, highly-oriented crystals, and extended-crystals are formed during the ultra-drawing of UHMWPE, which corresponds to the additional melting peak observed in this study. The molecular orientation of UHMWPE subsequently imparts improved tensile properties to the drawn films, which will be discussed later.

Table I. Thermal Properties of the UHMWPE Polymer Blend Systems with Different Compositions and Draw Ratios

LLDPE (%)	EPM (%)	Draw Ratio	T_m (°C)	T_c (°C)	H_m (J/g)	H_c (J/g)
0	0	0	143.4	100.7	204.5	116.54
5	0	0	146.8	96.4	209.6	120.5
10	0	0	144.3	99.0	164.4	95.3
20	0	0	142.4	95.1	206.3	138.4
30	0	0	140.2	95.1	221.3	145.3
0	5	0	145.1	99.2	227.9	132.3
0	10	0	145.8	99.8	245.4	145.6
0	20	0	145.0	101.9	262.5	156.2
0	30	0	146.9	97.1	230.0	130.95
5	0	100	142.9	106.5	205.4	-
5	0	200	144.8	105.3	223.2	-
5	0	300	143.9	104.6	224.6	-

Figure 2 compares the WAXD patterns of various UHMWPE blend systems. The WAXD patterns show diffraction peaks at $2\theta=21°$ and $2\theta=24°$ corresponding to the (110) and (200) planes respectively, which can be ascribed to the orthorhombic crystal structure of UHMWPE. As shown in Figure 2(a) and (b), when the low molecular-weight polymers are included in UHMWPE, the relative intensity of the (200) and (110) planes appears to decrease. The WAXD peaks are influenced more significantly by the addition of crystal defects of EPM. On the other hand, when the UHMWPE/LLDPE (5%) film is drawn, as shown in Figure 2(c), the peak corresponding to the (200) plane increases with increasing draw ratios, which compares well with previous work showing that the (200) plane orientation is preferable in the drawing process.[40]

Figure 3 shows polarized microscopic photographs of the UHMWPE/LLDPE (5%) blend film surfaces at different draw ratios. As the draw ratio is increased over 100 in Figure 3(c), the film surfaces appear to split in the vertical direction leaving permanent split lines. The number of the film splits increases with increasing draw ratio, and the split lines are ultimately interconnected at a draw ratio of 300 (Figure 3(e)). We believe that the formation of these split lines are similar to the necking process of polymeric materials often occurring when they are under a large tensile deformation. Although the area of the split lines is relatively small, the effect of the split lines on the porosity and gel-film performance should be further investigated.

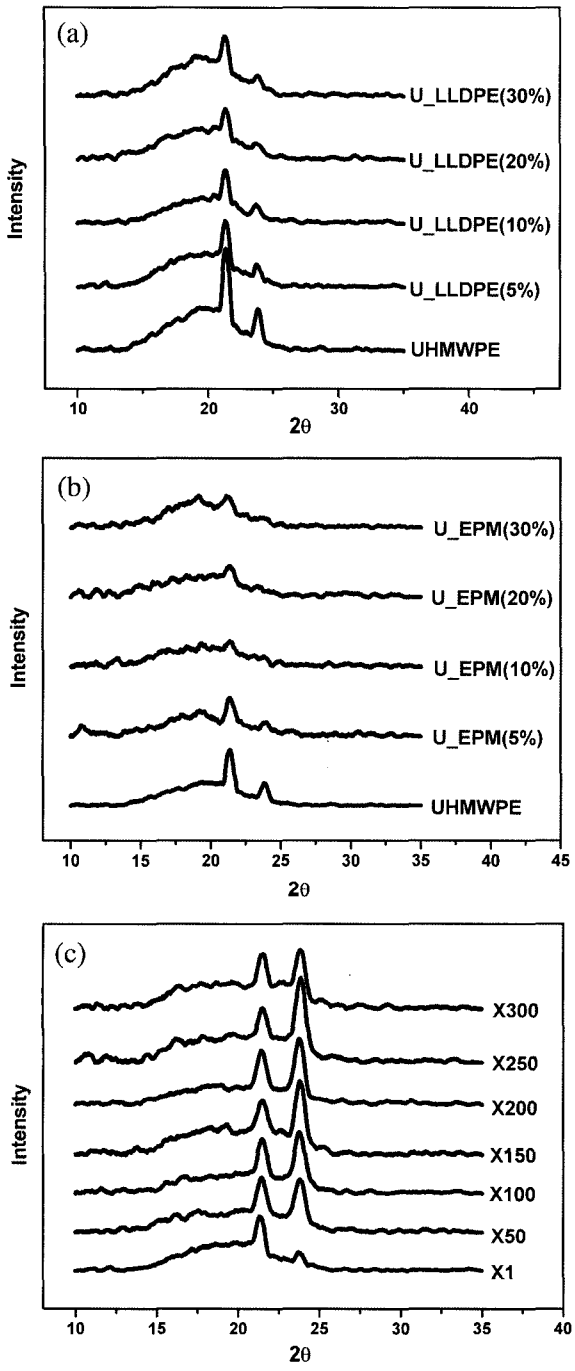

Figure 2. X-ray diffractograms of the UHMWPE/low molecular-weight polymer blend films at various compositions of (a) LLDPE at DR=1 and (b) EPM at DR=1, and (c) HWMWPE/LLDPE (5%) drawn at different drawing ratios.

When the gel solutions are at the critical concentration, they can be regarded as containing the correct level of entanglements between the UHMWPE crystal lamellae.[41-43] These entanglements play an important role in the transmission of the drawing force because they act as intermolecular

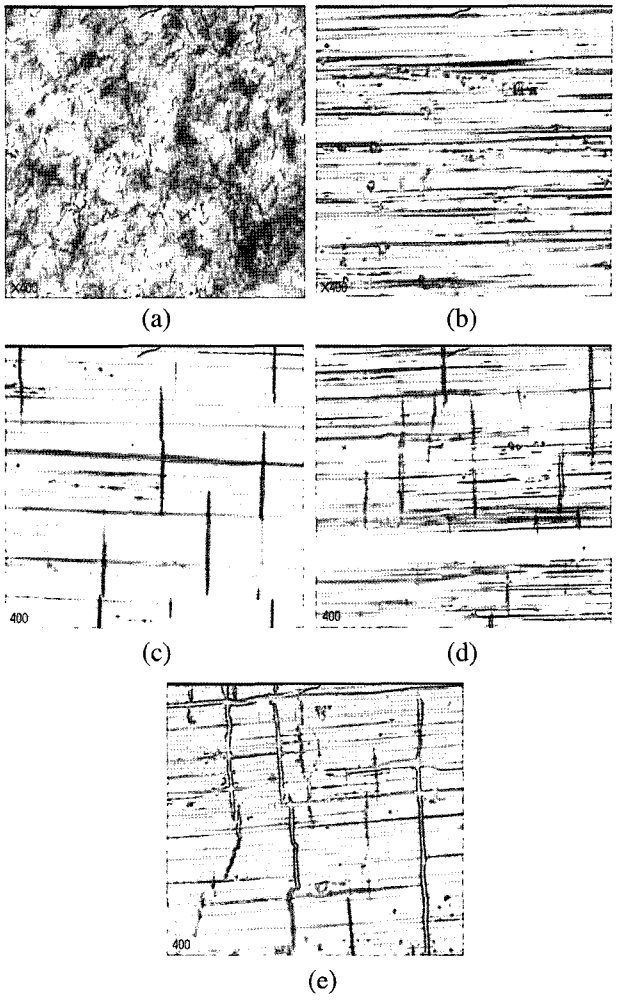

Figure 3. Polarized optical micrographs of UHMWPE/LLDPE (5%) blend film surfaces at different draw ratios of (a) 1, (b) 50, (c) 100, (d) 200, and (e) 300.

cross-linkers. As shown in Figure 4, the maximum draw ratio achievable at different compositions of a low molecular-weight polymer decreases with the increasing content of low molecular weight polymer. It is believed that the low molecular-weight polymers decrease the degree of chain entanglements and subsequently deteriorate the drawability of the gel films. A comparison of Figure 4(a) and (b) shows that the drawing temperature significantly increases the drawability of the gel films due to the enhanced chain mobility.

Figure 5 shows the tensile strength and modulus of the UHMWPE/LLDPE (5%) polymer blend films plotted as a function of the draw ratio. The tensile strength and the modulus of the undrawn films were 24 MPa and 1.8 GPa, respectively, which increase linearly with increasing draw ratio, reaching 750 MPa and 6 GPa, respectively, at a draw ratio of 300. This remarkable increase in the mechanical properties of the films is mainly due to the molecular orien-

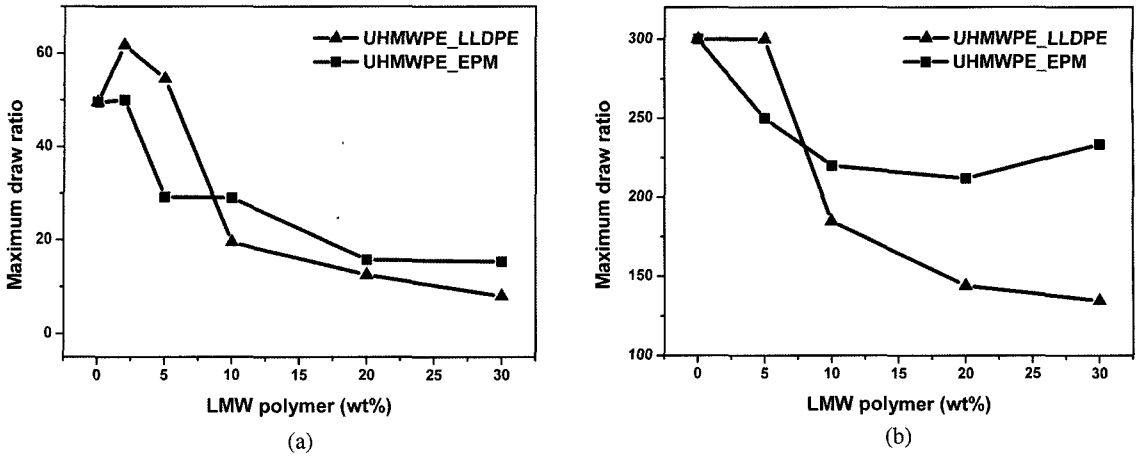

Figure 4. Maximum draw ratio of UHMWPE/low molecular-weight polymer blend films at various low molecular-weight compositions drawn at temperatures of (a) 50 °C and (b) 110 °C.

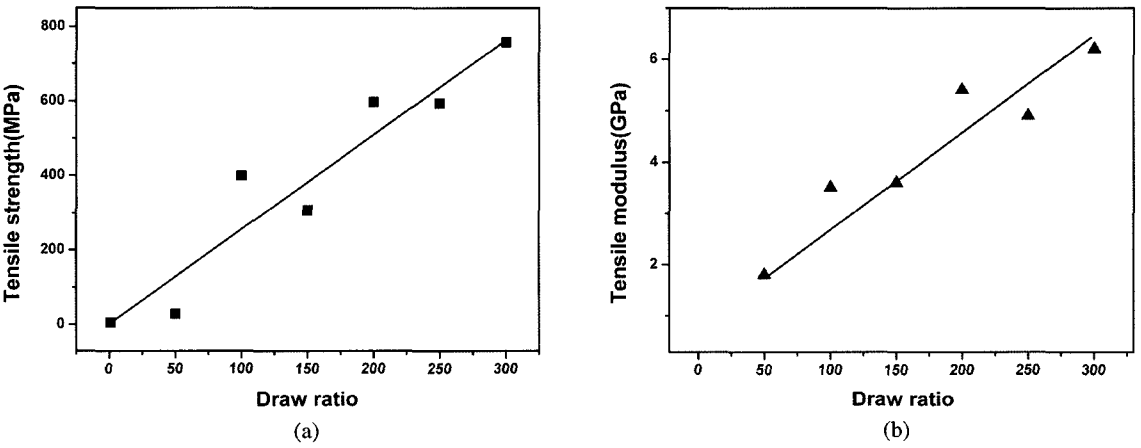

Figure 5. (a) Tensile strength and (b) modulus of gel-drawn films of UHMWPE/LLDPE (5%) polymer blend measured as a function of draw ratio.

tation of the polymer chains in the (200) planes, as shown in Figure 1(c) and Figure 2(c).

Figure 6 shows a comparison of the fractured surfaces of the undrawn films of the pristine UHMWPE and the UHMWPE/LLDPE (5%) blend. The pristine UHMWPE shows well-dispersed tiny fibrils and a relatively smooth fracture surface. On the other hand, the UHMWPE/LLDPE (5%) blend system has a relatively rough fracture surface with the UHMWPE fibrils appearing to be glued together to form a planar-web feature. When the UHMWPE gels are dried, the UHMWPE forms a randomly oriented fibril structure. This is apparently due to its extremely high molecular weight and long chain length, which is not the case with LLDPE. When LLDPE is incorporated into UHMWPE in the dry-gel state, there is a high probability that LLDPE does not form a fibril structure but resides with the UHMWPE fibrils acting as a binder. The morphological development of UHMWPE/LLDPE blend systems can be seen more clearly when heterogeneous nanoparticles ($BaTiO_3$) are included in the polymer systems.

Figure 7 shows SEM micrographs of $BaTiO_3$ composite systems containing different matrices: the pristine UHMWPE and the UHMWPE/LLDPE (5%) blend system. When the pristine UHMWPE is used as the matrix for the $BaTiO_3$ nanoparticles, as shown in Figure 7(A) and (B), the tiny nanofibrils of UHMWPE are well developed and the $BaTiO_3$ nanoparticles are also well dispersed. On the other hand, when LLDPE is blended with UHMWPE in the matrix, as shown in Figure 7(C) and (D), the UHMWPE fibrils appear to be bound together by the LLDPE to form a planar web feature. Consequently, particle dispersion appears relatively poor in the UHMWPE/LLDPE blend sys-

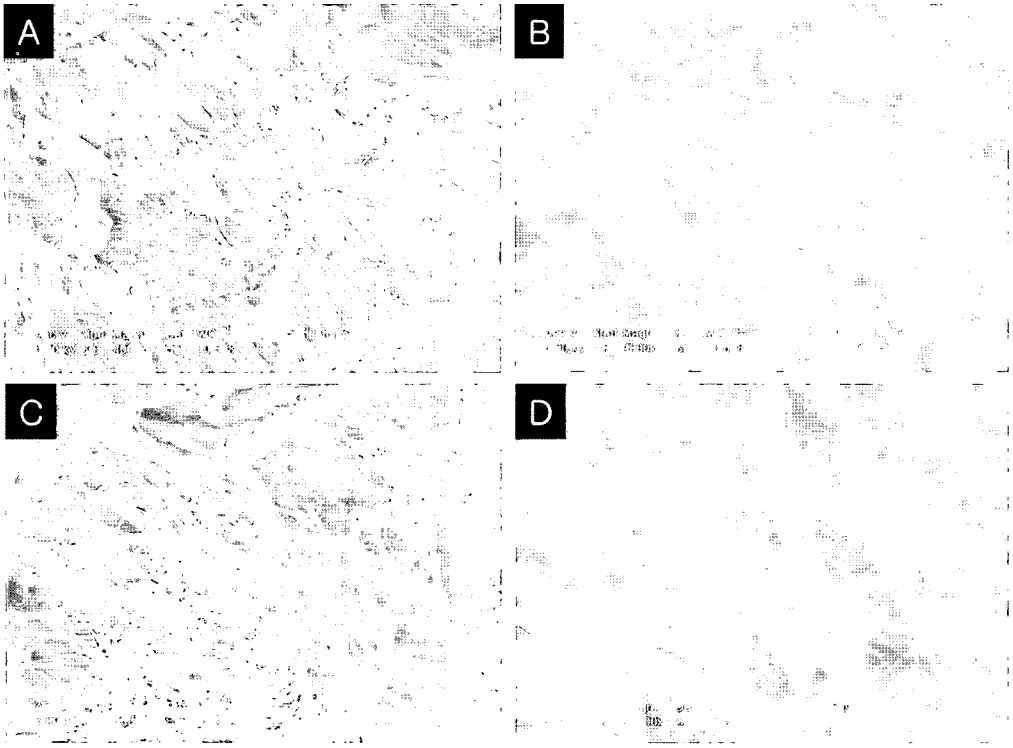

Figure 6. SEM images of the fractured surfaces of pristine UHMWPE (A and B at different magnifications) and UHMWPE/LLDPE (5%) composite specimens (C and D at different magnifications).

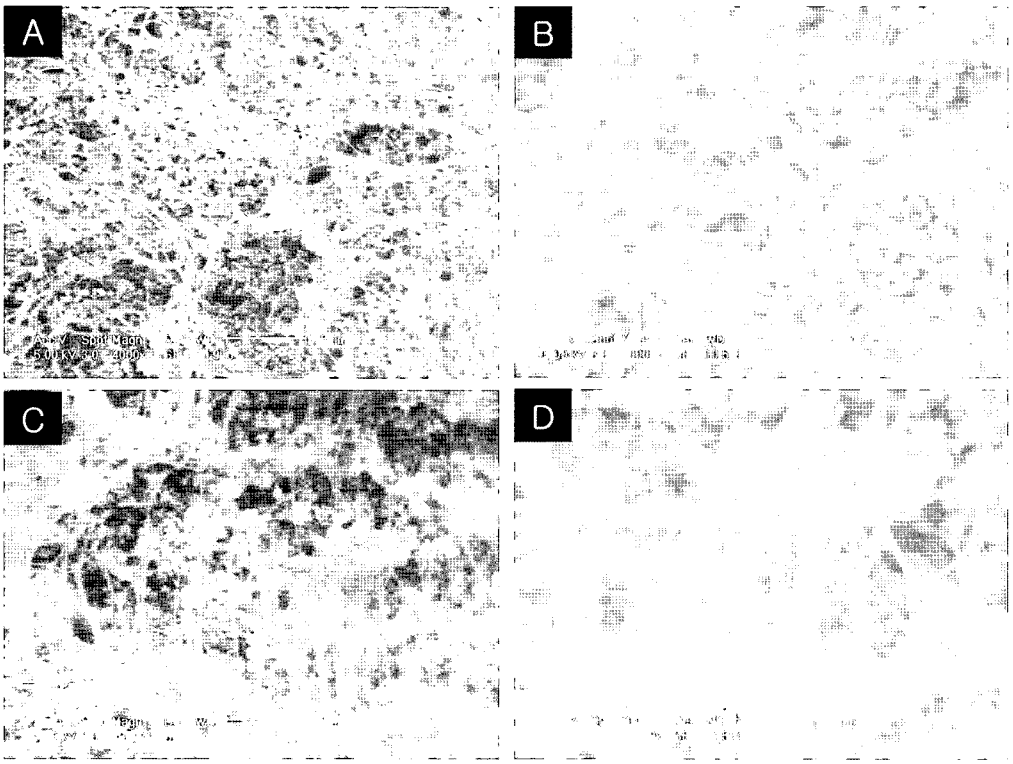

Figure 7. SEM images of UHMWPE/$BaTiO_3$ (A and B at different magnifications) and UHMWPE/LLDPE(5%)/$BaTiO_3$ (C and D at different magnifications) composite specimens without drawing (DR=1).

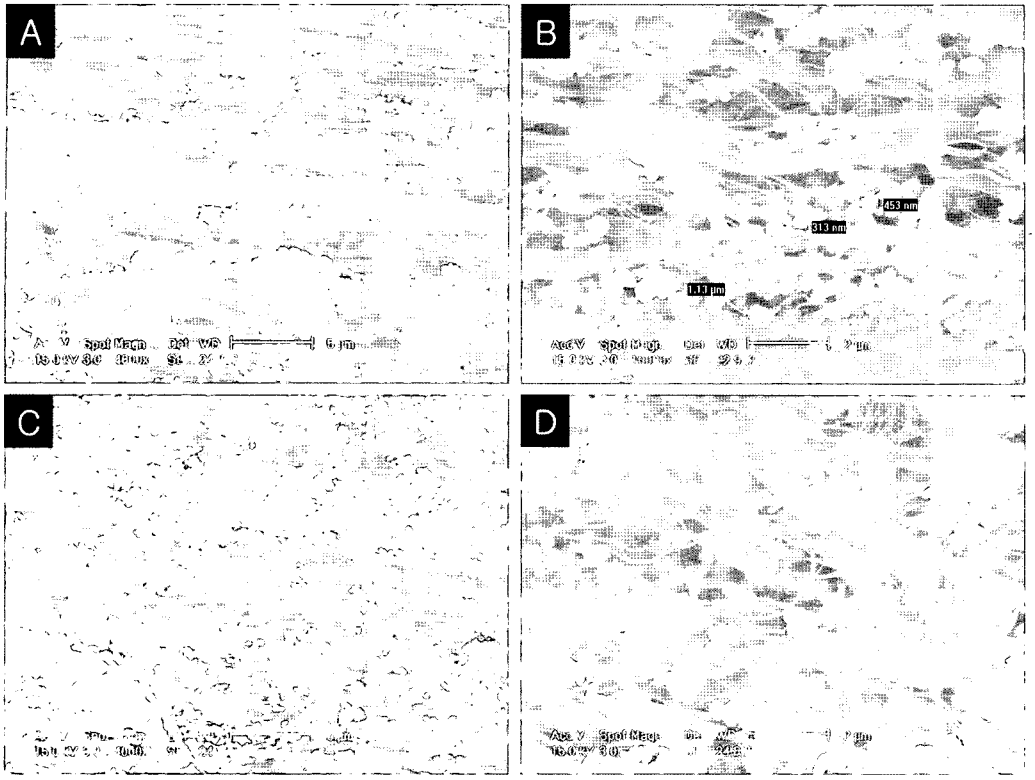

Figure 8. SEM images of UHMWPE/LLDPE (5%)/$BaTiO_3$ composite films with draw ratios of 30 (A and B at different magnifications) and 60 (C and D at different magnifications).

tem. Although the particle dispersion is poor in this stage of the dried-gel film, when the film is drawn to a large extent, the UHMWPE and LLEPE are further elongated in the drawing direction, which would further facilitates the nanoparticle dispersion.

Figure 8 shows the UHMWPE/LLDPE(5%)/$BaTiO_3$ composite films drawn at draw ratios of 30 and 60 in the horizontal direction of the figure. Comparing Figure 7 with Figure 8 before and after the drawing process, respectively, the aggregate size of $BaTiO_3$ particles is substantially decreased by the drawing process. However, clustered-nanoparticle aggregates can still be seen for a draw ratio of 30 in the range of few micrometers (Figure 8(A) and (B)). The UHMWPE nanofibrils aligned in the draw direction appear to be bound with the thin LLEPE film layers (Figure 8(B)). However, for a draw ratio of 60, no particulate aggregates, which can be seen in Figure 8(A) and (B), were observed, as shown in Figure 8(C) and (D). It is believed that the distance between the nanoparticles increases under the elongational deformation of the UHMWPE fibrils to facilitate the nanoparticle dispersion. In addition, the thin LLDPE film layers, which are likely to bind the UHMWPE nanofibrils together at a draw ratio lower than 30, disappear in the extended films at a draw ratio of 60. Conclusively, the ultra-drawing process of UHMWPE/LLDPE dry-gel films can be used to provide a highly-porous membranes containing highly-loaded and well-dispersed nanoparticles.

Conclusions

The gel-film drawing process of UHMWPE was investigated by incorporating low-molecular weight polymers and $BaTiO_3$ nanoparticles. The crystalline melting and recrystallization behavior of the UHMWPE/low molecular-weight polymer films were not significantly influenced by the physical blending. However, an additional crystalline melting peak was detected in the samples produced by the ultra-drawing process, which could be ascribed to the highly-oriented or highly-extended crystals of UHMWPE. The maximum draw ratio of the UHMWPE/low molecular-weight systems was 300, and the tensile strength and modulus of the drawn films reached 750 MPa and 6 GPa, respectively. The gel-drawn UHMWPE films exhibited nano-sized UHMWPE fibril structures glued with the LLDPE layers, which ultimately disappeared when the films were extended over a draw ratio of 60. The highly porous UHMWPE fibril structure could disperse a large amount of nano-sized inorganic particles.

Acknowledgements. This work was supported by the

Korea Research Foundation Grant (KRF-2004-005-D00063). We also appreciate technical and instrumental support from Samsung Electro-Mechanics Co. through research project to RIC in Sungkyunkwan University.

References

(1) A. Zwijnenburg and A. Pennings, *J. Colloid Polym. Sci.*, **254**, 868 (1976).
(2) P. Smith, P. J. Lemstra, and H. C. Booij, *J. Polym. Sci.; Part B: Polym. Phys.*, **19**, 877 (1981).
(3) M. Matsuo and R. S. Manley, *Marcromoecules*, **15**, 985 (1982).
(4) M. Matsuo and R. S. Manley, *Macromolecules*, **16**, 1505 (1983).
(5) C. Sawatari, T. Okumura, and M. Matsuo, *Polymer*, **18**, 741 (1986).
(6) T. Kanamoto, A. Tsuruta, K. Tanaka, M. Takeda, and R. S. Poter, *Polymer*, **15**, 327 (1983).
(7) T. Kanamoto, A. Tsuruta, K. Tanaka, M. Takeda, and R. S. Porter, *Macromolecules*, **21**, 470 (1988).
(8) H. Uehara, M. Nakae, T. Kanamoto, A. E. Zachariades, and R. S. Porter, *Macromolecules*, **32**, 2761 (1999).
(9) D. H. Yang, G. H. Yoon, G. J. Shin, S. H. Kim, J. M. Rhee, G. Khang, and H. B. Lee, *Macromol. Res.*, **13**, 120 (2005).
(10) G. Karay and M. J. Bevis, *J. Polym. Sci.; Part B: Polym. Phys.*, **35**, 263 (1997).
(11) P. Smith and P. J. Lemstra, *J. Colloid Polym. Sci.*, **258**, 89 (1980).
(12) T. Kanamoto, A. Tsuruta, M. Tanaka, and R. S. Porter, *Polym. J.*, **15**, 327 (1983).
(13) T. Kanamoto, S. Kiyooka, Y. Tovmasyan, H. Sano, and H. Narukawa, *Polymer*, **31**, 2039 (1990).
(14) S. S. Han, W. S. Yoon, J. H. Choi, S. Y. Kim, and W. S. Lyoo, *J. Appl. Polym. Sci.*, **66**, 1583 (1977).
(15) W. S. Lyoo, S. S. Han, J. H. Choi, Y. W. Cho, and W. S. Ha, *J. Korean Fib. Soc.*, **32**, 1023 (1995).
(16) T. Kunugi and I. Akiyama, *Polymer*, **23**, 1199 (1982).
(17) P. D. Garrett and D. T. Grubb, *Polym. Commun.*, **29**, 60 (1988).
(18) T. Kunugi, T. Kawasumi, and T. J. Ito, *J. Appl. Polym. Sci.*, **40**, 2101 (1990).
(19) P. Smith, P. J. Lemstra, and J. P. L. Pijpers, *J. Polym. Sci.; Part B: Polym. Phys.*, **20**, 2229 (1982).
(20) M. A. Hallam, D. L. M. Cansfield, I. M. Ward, and G. Pollard, *J. Mater. Sci.*, **21**, 4199 (1986).
(21) C. W. M Bastiaansen, *J. Polym. Sci.; Part B: Polym. Phys.*, **28**, 1457 (1990).
(22) B. L. Liu, N. Murakami, M. Sumita, and K. Kiyasaka, *J. Polym. Sci.; Part B: Polym. Phys.*, **27**, 2441 (1989).
(23) T. Ogita, N. Suzuki, and Y. Kawahara, *Polymer*, **33**, 698 (1992).
(24) T. Ogita, Y. Kawahara, Y. Soga, and M. Matsuo, *Colloid Polym. Sci.*, **270**, 833 (1992).
(25) R. W. Nunes, J. R. Marhn, and J. F. Johnson, *Polym. Eng. Sci.*, **22**, 205 (1982).
(26) M. J. F. Douglas and F. Freed, *Macromolecules*, **16**, 741 (1983).
(27) J. Yeh and H. Wu, *Polymer*, **30**, 1 (1998).
(28) M. Mihailov and L. Minkova, *Colloid Polym. Sci.*, **265**, 681 (1987).
(29) C. Sawatari and M. Matsuo, *Polymer*, **30**, 1603 (1989).
(30) Y. Bin, M. Fukuda, H. Kurosu, and M. Matsuo, *Macromol. Symp.*, **141**, 1 (2000).
(31) J. T. Yeh, Y. L. Lin, and C. C. Fan-Chiang, *Macromol. Chem. Phys.*, **197**, 3531 (1996).
(32) J. T. Yeh, S. S. Chang, and M. S. Yen, *J. Appl. Polym. Sci.*, **70**, 149 (1998).
(33) N. Nakajima and J. Ibata, *Jpn. Pats.*, 57,177,035 (1983).
(34) I. Simeonov, Z. Nililova, P. Komitov, and K. Naidenova, *Bulg. Pat.*, **31**, 868 (1982).
(35) M. Datta, T. Osaka, and J. W. Schultze, *Microelectronic Packaging*, CRC Press, New York, 2004.
(36) R. R. Tummala, *Fundamentals of Microsystems Packaging*, McGraw-Hill, New York, 2001.
(37) T. Ogita, A. Takada, T. Yamamoto, A. Kawaguchi, and S. Murakami, *Polymer*, **36**, 2181 (1995).
(38) H. Sakami, T. Izushi, and S. Iida, *Kobunshi Ronbunshu*, **38**, 103 (1981).
(39) H. Sakami, S. Iida, and K. Sasaki, *Kobunshi Ronbunshu*, **36**, 36 (1979).
(40) Y. Sakai and K. Miyasaka, *Polymer*, **29**, 1608 (1988).
(41) D. Darras, R. Sequela, and F. Rietsch, *J. Polym. Sci., Part B: Polym. Phys.*, **30**, 349 (1992).
(42) T. Ogita, R. Yamamoto, N. Suzuki, F. Ozaki, and M. Matsuo, *Polymer*, **32**, 822 (1991).
(43) M. Matsuo and C. Kitayama, *Polymer*, **17**, 479 (1985).